Deposit formation in a full-scale pulverized wood-fired power plant with and without coal fly ash addition

Wu, Hao; Shafique Bashir, Muhammad; Jensen, Peter Arendt; Sander, Bo; Glarborg, Peter

Published in:
Proceedings of 21st European Biomass Conference and Exhibition

Publication date:
2013

DEPOSIT FORMATION IN A FULL-SCALE PULVERIZED WOOD-FIRED POWER PLANT WITH AND WITHOUT COAL FLY ASH ADDITION

Hao Wu*[,1], Muhammad Shafique Bashir[1], Peter Arendt Jensen[1], Bo Sander[2], Peter Glarborg[1]
[1] Department of Chemical and Biochemical Engineering, Technical University of Denmark, Søltofts Plads, Building 229, DK-2800 Kgs. Lyngby, Denmark
[2] DONG Energy Thermal Power A/S, Kraftvæksvej 53, 7000 Fredericia, Denmark
* Corresponding Author. Phone:+45 4525 2927, Fax:+ 45 4588 2258, Email:haw@kt.dtu.dk

ABSTRACT: Ash transformation and deposition in a pulverized wood-fired power plant boiler of 800 MW_{th} were studied with and without the addition of coal fly ash. The transient ash deposition behavior was investigated by using an advanced deposit probe system at two different boiler locations with flue gas temperatures of ~1300°C and ~800°C, respectively. It was found that during pulverized wood combustion, the deposit formation at the high-temperature location was characterized by a slow and continuous growth of deposits followed by the shedding of a large layer of deposits, while the deposit formation at the low-temperature location showed a slow initial build-up and a stable mass of deposits after approximately 1-5 h. The deposits collected during pulverized wood combustion contained a considerable amount of K_2SO_4, KCl, and KOH/K_2CO_3. With the addition of coal fly ash (~4 times of the mass flow of wood ash) to the boiler, these alkali species were effectively removed both in the fly ash and in the deposits, and a more frequent shedding of the deposits was observed. The results imply that coal fly ash can be an effective additive to reduce ash deposition and corrosion problems in a pulverized wood-fired boiler.
Keywords: additives, alkali, fly ashes, fouling, boiler, biomass

1 INTRODUCTION

In order to secure the long-term goal of the Danish energy policy for achieving 100% renewable energy supply by 2050, one of the milestones is to phase out coal from Danish power plants by 2030, mainly by replacing coal with biomass in CHP plants and by promoting wind power [1]. Wood is considered as a feasible biomass for replacing coal in suspension-firing power plants, primarily due to its relatively small alkali and chorine content. However, a conversion from coal to wood on existing suspension-firing power plants may still involve a range of technical challenges for the boiler and the flue gas treatment units. Typical examples are the ash-related problems induced by the alkali metals and the chlorine present in wood [2,3], such as ash deposition [4,5], corrosion [5,6] and deactivation of SCR catalyst [7,8]. In order to facilitate the conversion from coal to wood on existing power plants, it is needed to have a systematic understanding of the ash transformation and deposition during pulverized wood combustion. Moreover, it is desirable to explore methods that could minimize the ash related problems, such as using additives [9]. Among the different additives that are usable in biomass combustion [9], coal fly ash has been proven to be effective in reducing the aerosol formation during pulverized wood combustion [10]. However, the effect of coal fly ash addition on ash deposition during pulverized wood combustion is not well-resolved.

The objectives of this work were to characterize and understand ash transformation and deposition during full-scale pulverized wood combustion, and to investigate the effect of coal fly ash addition on these processes. It was achieved by conducing ash deposition measurements at the Avedøre Power Plant Unit 2 (AVV2) by using an advanced deposit probe system. The influence of different boiler locations and operation conditions on deposit formation was studied. The ash transformation and deposition mechanisms were elaborated through characterizations of the collected deposit and fly ash samples along with analyses of deposit formation and shedding through recorded camera videos and boiler operation data.

2 EXPERIMENTAL

2.1 Boiler and measurement locations

The Avedøre Power Plant Unit 2 (AVV2) owned by DONG Energy Thermal Power A/S is located at the Copenhagen area of Denmark. The complete plant consists of a suspension-fired main boiler, a straw-fired grate boiler and two gas turbines [11]. The present study was carried out in the main boiler of AVV2, which is an ultra supercritical (USC) tower boiler of the Benson type. The 800 MW_{th} main boiler can be fired with wood pellets, natural gas and heavy fuel oil [11]. The lower part of the boiler consists of the combustion chamber with 16 tangential-fired burners in 4 levels. The highest burner level is gas-fired only, whereas the other three levels can be fired with pulverized wood supplied by three mills respectively.

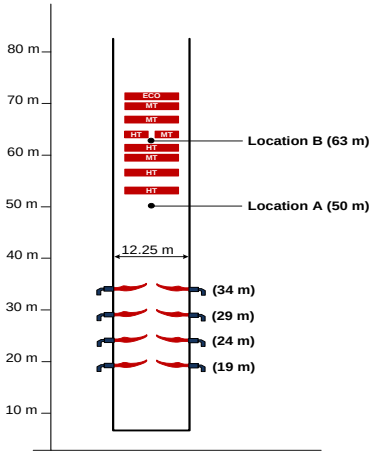

Figure 1: Simplified schematic drawing of the main boiler of AVV2 (HT: high temperature superheater, MT: medium temperature superheater, ECO:economizer). The height is based on the sea level.

A schematic drawing of the main boiler of AVV2 is shown in Figure 1. In this study, the ash deposition measurements were carried out at two different boiler locations. As illustrated in Figure 1, the first location

(denoted as Location A hereafter) is situated at a level of ~50m, which is just below the radiation shield of the boiler. The second location (denoted as Location B hereafter) is situated at a level of ~63m, which is in the superheater region of the boiler.

2.2 Fuels and additives

In the present work, the fuels fired in the boiler were wood and natural gas. The additive used was coal fly ash from a pulverized coal-fired power plant, which was injected to the AVV2 boiler through the nozzles at the two highest burner levels. The wood and the coal fly ash were sampled periodically throughout the measurements. Their average properties (based on a number of the analyzed samples) are shown in Table I. Wood ash content is very small, only about 1 wt% db. The major ash forming elements in wood are Ca, Si and K, whereas the content of Cl and S is low. Different from the wood, the coal fly ash is characterized by a large content of Si and Al. No Cl is found in the coal fly ash, while the S content is considerably larger than that of the wood. The natural gas used in the boiler is generally very clean with negligible content of the ash forming elements.

Table I: Properties of fuels and additives.

Properties	Wood	Coal ash
Ash contents (wt% ar)	0.99	--
Moisture (wt% ar)	6.76	--
LHV (MJ/kg ar)	17.51	--
S (wt% db)	0.017	0.26
Cl (wt% db)	0.0069	0
Al (wt% db)	0.024	14
Ca (wt% db)	0.208	5.2
Fe (wt% db)	0.020	2.3
K (wt% db)	0.091	0.45
Mg (wt% db)	0.034	0.91
Na (wt% db)	0.007	0.11
P (wt% db)	0.012	0.81
Si (wt% db)	0.17	20

2.3 Ash deposition probe system at Location A

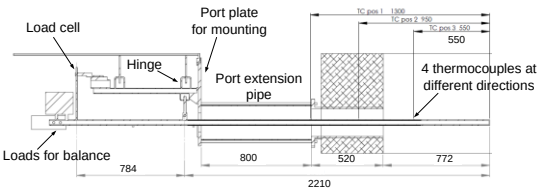

Figure 2: Schematic drawing of the probe system used at Location A of AVV2, modified from [13].

An advanced deposit probe system developed in our earlier studies [12-14] was adopted in this work. A drawing of the probe system used at Location A is shown in Figure 2. The deposit probe is made of stainless steel, about 3 m long and having an outer diameter of 40.5 mm. A load cell was mounted to continuously measure the deposit build-up on the probe. The probe was cooled by water and air, and it was possible to keep a stable surface temperature of the probe. At Location A, the probe was placed in an acoustic pyrometer port on the boiler wall. Due to the high flue gas temperatures at this location, it was not possible to keep the probe surface temperature between 500 and 600^{o}C when the probe was fully inserted. Therefore, a special port extension pipe was installed to keep the probe only 772 mm inside the boiler. This solution worked satisfactorily towards controlling the surface temperature of the probe to be around 550^{o}C. The thermocouple used for controlling the probe surface temperature was placed 550 mm from the tip of the probe, with an angular position facing the bottom of the boiler. In order to minimize the effect of soot blowing on the probe, the two nearest soot-blowers were shut off during the measurements.

The flue gas temperature near the probe was measured continuously by using an S-type thermocouple placed in a ceramic protective shell. In addition, a suction pyrometer (International Flame Research Foundation model, IFRF [15]) was used for some periods to find the difference between the flue temperatures measured by the ceramic S-type thermocouple and the suction pyrometer.

A special port used for video monitoring was mounted at the wall right-side of the probe measurement position. The port was cooled by water and air, and a CCD (charge-coupled device) camera was placed in the port to register the deposit formation and removal processes on the probe. During some periods, an additional camera was placed below the probe for obtaining a better understanding of the ash deposition processes. Both cameras took pictures continuously with constant intervals of 10 s.

2.4 Ash deposition probe system at Location B

The probe system used at Location B was slightly different from that of Location A. Due to the low flue gas temperatures, the deposit probe was fully (1400 mm) inside the boiler at Location B. Again, the two soot-blowers near-by the probe were shut off to minimize the effect of soot blowing. Since there was no extra opening available near-by the probe, the flue gas temperature was measured at the wall opposite of the probe, by using a K-type thermocouple placed in a metallic protective shell and the suction pyrometer mentioned above. Due to the small size (80 mm in diameter) of the opening for the deposition probe and the lack of other near-by openings, camera monitoring was not possible at Location B.

2.5 Experimental matrix

Table II: Experimental matrix.

Exp.	Posit.	Time (h)	Boiler load (%)	Biomass load (%)	Coal ash (ton/h)	Coal ash/ wood ash
1	A	100.8	92.1	83.1	-	-
2	B	40.3	80.5	71.8	-	-
3	B	23.6	96.3	86.7	6	4.1
4	A	25.5	93.4	78.2	5.8	4.4
5	A	18	85.7	78.9	6	4.5
6	A	25.1	82.8	73.2	5.7	4.6
7	A	26	91.2	44.1	2.7	3.6
8	A	16	97.6	81.2	6.0	4.4
9	A	28	88.5	72.2	5.7	4.7
10	A	116	41.4	18.2	2.3	7.4
11	A	52	76.3	59.2	5.8	5.8

An overview of the performed tests is shown in Table II. It can be seen that the tests were carried out at two locations both with and without coal fly ash addition. In most of the tests, the boiler was kept at a high load (above 80%) and wood was the dominant fuel. However,

there were a few tests (Test 10 and 11) where the boiler load was relatively low. For most of the tests with coal fly ash addition, the mass ratio of the added coal fly ash and the wood ash was around 4.5. However, a higher coal fly ash to wood ash ratio was applied for Test 10 and 11. During the experiments, the target probe temperature was 550°C, while the actual probe surface temperature varied slightly during the experiments.

2.6 Data treatment

Based on the load-cell signal of the probe, the deposit mass uptake on the probe can be calculated by using the following torque balance:

$$m_d = (m_{t0} - m_{t1})\frac{L_1}{L_2} \quad (1)$$

where m_d is the deposit mass (g), m_{t0} is the initial signal of the load cell (g), m_{t1} is the final signal of the load cell (g), while L_1 and L_2 are the distances (mm) from the hinge to the balance and to the mass center of the deposit, respectively.

With the deposit mass uptake data, the surface area of the probe exposed to the flue gas and the corresponding exposure time, the ash deposition rate (g/m^2/h) can be calculated. In this study the derivative based-deposit formation rate (DDF-rate) defined in our earlier work [13,14] is used to characterize the deposit formation. The detailed procedure for calculating the DDF-rate is described elsewhere [13]. In brief, the DDF-rate is calculated by taking the time derivative of the deposit mass uptake in-between two major shedding events. Therefore it represents a deposit formation rate, which is an averaging of the time derivative over periods that do not include major shedding events, but do include some minor shedding events in addition to noise. Using the DDF-rate, the ash deposition propensity can be calculated by the following equations:

$$Ash\,deposition\,propensity = \frac{DDF\text{-}rate}{Ash\,flux} \quad (2)$$

$$Ash\,flux\ (g/m^2/h) = \frac{m_f X_a}{A_r} + \frac{ash_{coal}}{A_r} \quad (3)$$

where m_f is the wood flow to the boiler (g/h), X_a represents wood ash fraction, ash_{coal} is the coal ash flow (g/h) and A_r is the cross-sectional area of the boiler at the probe measuring position. The mass flow rate of the fuels and the coal fly ash as well as a number of other boiler operation parameters were recorded continuously throughout the measurement periods.

In the calculation of the DDF-rate, a cut off level of -3800 g/m^2/h was chosen to identify the major shedding events [13]. By using this criterion, the number of the major shedding events during a certain time period can be obtained through the procedures described in [14]. In addition, the frequency of the shedding events (hr^{-1}) and the mean deposit mass drop (g/m^2) of the shedding events during the time period can also be calculated.

It is seen in Table II that the duration of the tests is quite different. Besides, for some long-period tests, the operation parameters varied considerably within the test. In order to compare the results under similar duration and meanwhile take into account the possible parameter fluctuations in a long-period test, each of the performed tests is divided into sub-tests with a duration of approximately 6 hours (e.g. Test 3 is divided into 4 sub-tests). The average ash deposition data in these sub-tests are calculated and compared. This treatment allows us to study the influence of the fluctuation of operational parameters within a test. It should be noted that a few unexpected problems occurred during some of the tests (e.g. shut-off of cooling water and loss of load-cell signal). The experimental periods influenced by these problems are carefully identified and are excluded when presenting the results.

2.7 Deposit/ash sampling and analysis

The deposits on the probe were collected after each test. At Location A, the collected deposits were divided into three fractions, namely outer layer windward deposits, inner layer windward deposits, and leeward deposits. The deposits collected on the half-circle facing the bottom of the boiler were denoted as windward deposits. The outer layer windward deposits were large pieces of deposits which were easily removed by using a glass stick. The inner layer windward deposits or the leeward deposits contained condensed species that were more difficult to remove. Thus a metal brush was used to collect these deposits. At Location B, the collected deposits were simply divided into windward deposits and leeward deposits, since the formation of large outer layer deposits was not observed. The deposit samples chosen for analysis were from Test 1–4, which were believed to be representative for the other tests under similar conditions. Besides the deposits, fly ash samples were collected periodically from the electrostatic precipitator (ESP) of the boiler during the measurement periods.

The fly ash samples were analyzed by SEM-EDS (Scanning Electron Microscopy and Electron Dispersive X-rays Spectroscopy) and XRD (X-ray Diffraction). In addition, the bulk/water soluble inorganic composition of the fly ash was analyzed by ICP-OES (Inductively Coupled Plasma Optical Emission Spectroscopy) or IC (Ion Chromatography). The collected deposits were also analyzed by SEM-EDS and ICP-OES/IC for the bulk/water soluble inorganic composition.

3 RESULTS AND DISCUSSION

3.1 Overview of the tests

An overview of the operation conditions during the tests is shown in Table III. The consistent oxygen level in the flue gas suggests that the tests are conducted under similar stoichiometric conditions. The CO concentrations are generally small, indicating a high level of burnout in the tests. The concentrations of SO_2 in the flue gas are negligible during the tests of pulverized wood combustion (Test 1, 2), implying that the S in wood is predominantly transformed to sulfates. This hypothesis is supported by a considerable amount of alkali sulfates found in the aerosols from wood combustion in the same boiler [10]. With the addition of coal fly ash (Test 3–11), the concentration of SO_2 is mostly increased to a level of about 5-15 ppm. This implies that reactions may have taken place between the gaseous alkali sulfates and the added coal fly ash, which generate alkali aluminosilicates and release SO_2 to the flue gas. Another possibility is that most of the gaseous alkali species (e.g. KCl and KOH) released from wood may have reacted with the added coal fly ash, thus limiting their conversion to sulfates through reactions with SO_2/SO_3. Besides the effect of coal fly ash addition, the SO_2 concentration in the present

study seems to be also influenced by the biomass load. For the tests with a low biomass load (Test 7 and 10), the SO_2 concentration in the flue gas is very low in spite of the high coal fly ash to wood ash ratio. A possible explanation is that reactions of coal fly ash and the gaseous alkali species may be inhibited at lower temperatures [16], which are influenced by the fuel/biomass load.

Table III: Summary of experimental conditions.

NO.	Posit.	Ash flux ($g/m^2/h$)	CO (ppm)	O_2 (%)	SO_2 (ppm)	Flue gas T. (^oC)[a]	Probe T (^oC)[b]
1	A	11296	86	3.0	0	1275	534
2	B	9756	40	3.0	0	783	515
3	B	59689	7	3.0	14.5	768	527
4	A	57277	18	3.0	12.7	1269	568
5	A	58600	37	3.1	14.7	1260	530
6	A	55150	29	3.1	15.5	1319	575
7	A	28886	48	2.4	0.3	1350	577
8	A	58782	5	2.8	4.8	1250	583
9	A	54931	37	2.9	8.2	1300	561
10	A	20580	1	3.2	0	950	483
11	A	45571	20	3.0	4.3	1075	525

[a] The flue gas temperature at the location of the probe is directly measured by suction pyrometer or by correcting the temperature measured by thermocouple (S/K type) with the mean difference found between the thermocouple and suction pyrometer measurements. [b] Average temperature of the four thermocouples placed at the same axial position (550 mm from the tip of the probe) but different radial positions of the probe is used.

The ash flux during different tests is given in Table III.. It is seen that for the tests with coal fly ash addition, the ash flux is typically much larger (up to 5-6 times) than that of the tests without coal fly ash addition (Test 1, 2). The average flue gas temperatures at the probe location and the average probe surface temperature during the tests are listed. It is seen that the flue gas temperature at Location A is in a range of 1250-1350^{o}C when the boiler is at operated at a high load (>80%). However, at a lower load (Test 10 and 11), the temperatures at Location A is decreased accordingly. Compared to Location A, the flue gas temperature at Location B is considerably lower, typically only around 770-800^{o}C. For most of the tests, the surface temperature of the probe is reasonably well-controlled to be around 550^{o}C. An exceptional case is Test 10, where the average surface temperature of the probe is only around 480^{o}C.

3.2 Properties of the fly ash

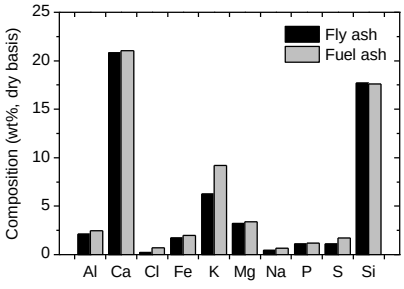

Figure 3: Compositions of the ESP fly ash during pulverized wood combustion (Test 1 and 2) and the fuel ash compositions of wood derived from Table I.

The bulk compositions of the ESP fly ash collected from pulverized wood combustion (Test 1 and 2) are shown in Figure 3, along with the compositions of wood ash derived from Table I. It is seen that the fly ash from pulverized wood combustion contains primarily Ca, Si and K, which generally represents the fuel ash composition. Compared to the fuel ash, the content of K, Cl and S is considerably smaller in the fly ash, which may be because a large fraction of KCl and K_2SO_4 presented in the flue gas has been deposited in the boiler.

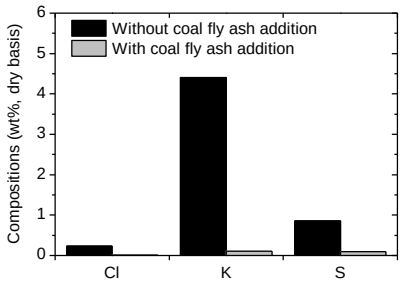

Figure 4: Water soluble compositions of the fly ash collected at the electrostatic precipitator (ESP) during the tests without coal fly ash addition (pulverized wood combustion) and the tests with coal fly ash addition.

The content of water soluble K, Cl and S in the ESP fly ash from pulverized wood combustion is shown in Figure 4. A comparison with the bulk fly ash composition reveals that approximately 80% of the S and 70% of the K in the fly ash are water soluble, and the Cl is totally water soluble. The molar ratio of the water soluble K/(Cl+2S) is about 1.9, indicating that only part of the water soluble K is comprised of KCl and K_2SO_4, with the remaining possibly being KOH and/or K_2CO_3. The presence of KCl, K_2SO_4, KOH and K_2CO_3 in the wood fly ash is supported by the XRD analysis results shown in Figure 5a. In addition to the K species, the major crystalline phases in the fly ash are SiO_2 and CaO, along with small amounts of MgO and $CaCO_3$.

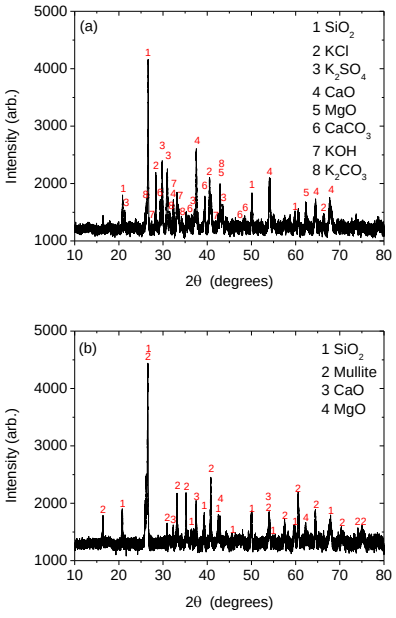

Figure 5: XRD analysis of the fly ash collected at the electrostatic precipitator (ESP) during (a) the tests without coal fly ash addition (pulverized wood combustion), (b) the tests with coal fly ash addition.

The addition of coal fly ash changes significantly the compositions of the fly ash collected at the ESP. As shown in Figure 4, the content of water soluble K, Cl and S becomes negligible in the collected ESP fly ash. The effect is obviously beyond the dilution effect caused by the added coal fly ash, indicating that reactions have taken place between the gaseous K species (e.g. KCl, K_2SO_4 or KOH) released from wood combustion and the added coal fly ash, leading to the formation of solid K-aluminosilicates and the release of gaseous products such as HCl and SO_2. Similar reactions between have been reported in a number of studies dealing with co-combustion of coal and high-alkali fuels [17-20].

According to Figure 5b, the major crystalline phases in the fly ash collected during coal fly ash addition are SiO_2 and mullite ($3Al_2O_3 \cdot 2SiO_2$), supplemented by small amounts of CaO and MgO. Almost no crystalline phase containing K-Al-Si or K-Si is seen from the XRD analysis, implying that either the amount of K-aluminosilicates or K-silicates is too small in the fly ash or they are in an amorphous phase that is not detectable by XRD. The latter explanation is advocated, since a large number of spherical particles rich in K, Al and Si are seen from SEM-EDS analyses of the fly ash particles (see typical examples in Figure 6).

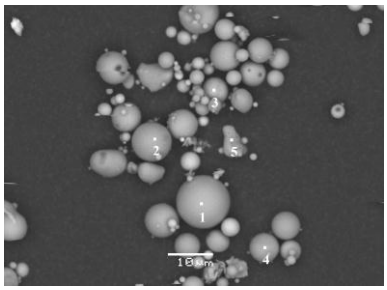

Figure 6: Typical SEM-EDS results of the ESP fly ash from the test with coal fly ash addition: K-Al-Si rich particles (spot 2-5), Ca-Al-Si rich particles (spot 1).

3.3 Qualitative observations of ash deposition

During the test of pulverized wood combustion without coal fly ash addition (Test 1), it is seen from the camera pictures that the formation of deposits is negligible at Location A in the period of 0-65 h. However, in the period of 65-100 h, the formation of deposits becomes obvious, particularly after 80 h. The observed different ash deposition behavior in the two periods is presumably related to the variation of wood properties, which is difficult to control for such a plant firing about 150 ton/h of wood. The analysis of the wood sample collected at the beginning of the test (0-10 h) shows a Cl content of 0.004 (wt% db) and an S content of 0.025 (wt% db). However, for the wood sample collected at the end of the test (90-100 h), the Cl content is increased to 0.018 (wt% db), whereas the S content is decreased to 0.018 (wt% db). Since other conditions (e.g. the flue gas temperature and the probe surface temperature) are quite consistent during the test, it is most likely that the increased formation of deposits in the later period of the experiment (65-100 h) is induced by an increased Cl content and a decreased S content in the wood.

The camera pictures show that the deposit formation during the period of 65-100 h at Test 1 is characterized by a slow and continuous growth which typically lasts about 5-10 h. The formed deposits is normally a thick layer with a typical example is shown in Figure 7a. The removal of deposits is also seen clearly from the camera pictures, with debonding (i.e. a large of layer of deposits is detached from the probe) as the main removal mechanism. A typical example of the deposits removal is shown in Figure 7a and Figure 7b, where the removal of a large layer of deposits is seen within a time interval of 10 s. Despite the two soot-blowers nearest the probe were closed during the tests, the removal of deposits is believed to be induced by the operation of other soot-blowers in the boiler, as the deposit removal occurred mostly within the operation periods of soot-blowers in the boiler. In addition, the observation from camera pictures indicates that the removal of deposits on the probe almost occurred the same time with the removal of wall deposits.

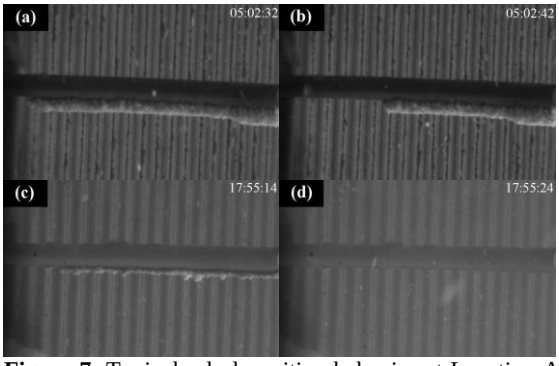

Figure 7: Typical ash deposition behavior at Location A during (a,b) the test (Test 1) without coal ash addition (pulverized wood combustion), (c,d) the test (Test 4) with coal ash addition.

With the addition of coal fly ash (Test 4-11), the ash deposition behavior at Location A is changed significantly. Compared to the test without coal fly ash addition, the deposit build-up rate becomes much faster and the shedding of deposit occurs more frequently when coal fly ash is added. A typical example is shown in Figure 7c, where the observed layer of deposits is formed within 20 min of exposure time. However, after 10 s, the deposit layer is completely removed through debonding (see Figure 7d). The frequency of deposit shedding during the tests with coal fly ash addition is much higher that the operation frequency of soot-blowers (normally in an interval of 5-20 h) in the boiler. Thus it is most likely that the shedding of deposits during the addition of coal fly ash is caused by natural shedding, rather than induced by soot-blowers.

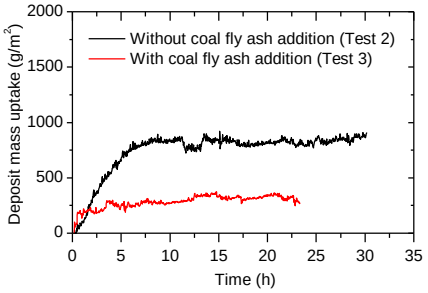

Figure 8: Deposit mass uptake during the tests (Test 2 and Test 3) at Location B.

Figure 8 shows the deposit mass uptake during the tests at Location B. For both tests, it can be seen that the deposit mass build-up is relatively slow and becomes almost constant after a few hours. Different from the tests at Location A where a lot of major shedding events are observed, the mass uptake at Location B does not show any major shedding event, both for the tests with and without coal fly ash addition. However, compared to the test without coal fly ash addition, it appears that the initial mass build-up is faster but the stabilized deposit mass uptake is smaller at Location B when coal fly ash is added.

3.4 DDF-rate and deposition propensity

The DDF-rate and the ash deposition propensity obtained from the different tests are plotted against the flue gas temperature in Figure 9 and Figure 10. The figures also give information about the average probe surface temperature during the tests. At Location A, it can be seen that the DDF-rate is usually not greater than 600 g/m^2/h during pulverized wood combustion without coal fly ash addition. With the addition of coal fly ash, the DDF-rate is increased, mostly to a level of a few thousands g/m^2/h. The increase of DDF-rate is partly because the ash flux in the flue gas is significantly increased when the coal fly ash is added (see **Error! Reference source not found.**). On the other hand, for the tests with high flue gas temperature (>1200^{o}C) and high probe surface temperature (>540^{o}C), the ash deposition propensity also becomes much higher when the coal fly ash is added (see Figure 10).

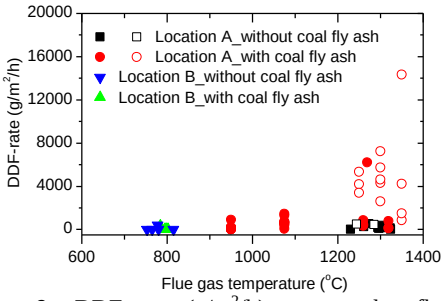

Figure 9: DDF-rate (g/m^2/h) versus the flue gas temperature (^{o}C) during different tests. The open symbols denote the test periods with a high average probe surface temperature (>560^{o}C), while the solid symbols denote the periods with low probe temperature (<540^{o}C).

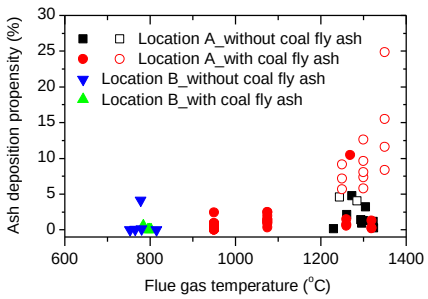

Figure 10: Ash deposition propensity (%) versus the flue gas temperature (^{o}C) during different tests. The open symbols denote the test periods with a high average probe surface temperature (>560^{o}C), while the solid symbols denote the periods with low probe temperature (<540^{o}C).

Compared to Location A, the DDF-rate and the ash deposition propensity at Location B are generally much lower. This is in-line with the deposit mass uptake profiles shown in Figure 8, where the deposit formation rate appears to be negligible after about 6 hours. For the test without coal fly ash addition, a data point with a relatively high ash deposition propensity (~5%) is seen in Figure 10, which corresponds to the initial build-up of deposits shown in Figure 8. However, for the test with coal fly ash addition, although the initial build-up appears to be fast (see Figure 8), the ash deposition propensity shown in Figure 10 is very low (<0.6%), mainly because the data is averaged over a period of 6 h (much longer than the initial build-up period) and the ash flux is much larger when coal fly ash is added.

3.5 Deposit removal frequency and mass-drop

The deposit removal frequencies versus the flue gas temperatures during different tests are shown in Figure 11. It can be seen that the deposit removal frequency at Location B is zero, both for the tests with and without coal fly ash addition. The results are consistent with the deposit mass uptake profiles shown in Figure 8, where no major deposit removal event is observed. At Location A, the deposit removal frequency during pulverized wood combustion is mostly below 0.5 hr^{-1}. However, with the addition of coal fly ash, the deposit removal frequency is typically increased to a level of around 2 hr^{-1}. This tendency is in agreement with the observations from the camera pictures, which have been discussed previously. For the tests with coal fly ash addition at Location A, the deposit removal frequency seems to be increased significantly when the flue gas temperature becomes higher than 1000^{o}C, while the effect of the probe surface temperature is not obvious. For the tests without coal fly ash addition, there is no obvious effect of the flue gas temperature and the probe surface temperature on the deposit removal frequency at Location A.

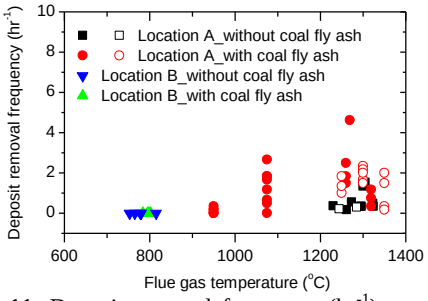

Figure 11: Deposit removal frequency (hr^{-1}) versus the flue gas temperature (^{o}C) during different tests. The open symbols denote the test periods with a high average probe surface temperature (>560^{o}C), while the solid symbols denote the periods with low probe temperature (<540^{o}C).

The average mass drop (g/m^2) during the deposit removal is plotted against the flue gas temperature in Figure 12. The data at Location B is excluded in the figure, as there is no major deposit removal event at this location. From the results it can be seen that the average deposit mass drop during pulverized wood combustion without coal fly ash addition is in a range of 100-650 g/m^2 at Location A. The average deposit mass drop during the tests with coal fly ash addition is dependent both on the flue gas temperature and the probe surface temperature. Under high flue gas temperature (>1200^{o}C) and high probe surface temperature (>560^{o}C) conditions, the average deposit mass drop is in a range of 1000-3000 g/m^2, which is considerably larger than that of the tests without coal fly ash addition. However, for the tests conducted at low flue gas temperature (<1200^{o}C) and/or

low probe surface temperature (<540°C), the average deposit mass drop is generally below 1000 g/m^2, which is comparable to the tests without coal fly ash.

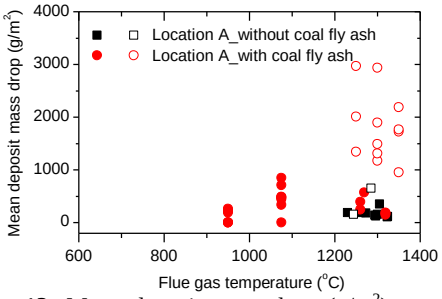

Figure 12: Mean deposit mass drop (g/m^2) versus the flue gas temperature (°C) during different tests. The open symbols denote the test periods with a high average probe surface temperature (>560°C), while the solid symbols denote the periods with low probe temperature (<540°C).

3.6 Deposit properties

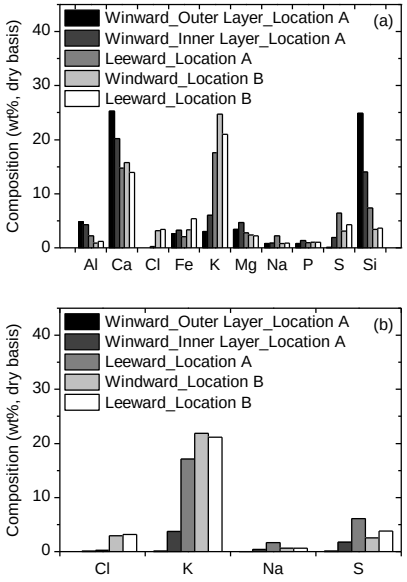

Figure 13: (a) Bulk compositions of the deposits collected during the tests without coal fly ash addition, (b) water soluble compositions of the deposits collected during the tests without coal fly ash addition.

Figure 13 shows the bulk and water soluble compositions of the deposits collected during the tests of pulverized wood combustion without coal fly ash addition. It can be seen that the outer layer windward deposits collected at Location A are enriched in Ca and Si, which largely represents the fly ash composition shown in Figure 3, except negligible S, Cl and water soluble K. SEM-EDS analyses suggest that the outer layer deposits are comprised mainly of spherical particles with relatively large Ca, Si and K content and with a size typically varying from ~5-100 μm (see typical examples from spot 1-2 and spot 4-9 in Figure 14a). Compared to the outer layer deposits, the inner layer windward deposits at Location A have slightly higher K and S content, with about 60% of the K and 90% of the S being water soluble. The molar ratio of the water soluble (K+Na)/2S in the inner layer deposits is about 1.01, suggesting that the water soluble alkalis are primarily alkali sulfates. SEM-EDS analyses (see typical examples in Figure 14b) show that the morphology of the inner layer deposits is not significantly different from the outer layer deposits, except the appearance of some sulfur-rich submicron particles that are attached to the surface of the large particles or being partially melted (see typical examples from spot 2 and spot 6 in Figure 14b). Compared to the windward deposits, the leeward deposits at Location A exhibit very different compositions. The dominant inorganic elements in the leeward deposits are Ca and K, supplemented by a considerable amount of S and Si. A small content of Cl (0.2 wt%) is also found in the leeward deposits. The majority (>95%) of the K, S and Cl in the leeward deposits appear to be water soluble. The molar ratio of the water soluble (K+Na)/(Cl+2S) is 1.36, indicating that the water soluble alkalis are not only sulfates and chlorides, but may also contain other water soluble alkali species (such as hydroxides or carbonates). The molar ratio of S/Cl in the leeward deposits is about 34, meaning that sulfates are dominant over chlorides. SEM-EDS analysis of the leeward deposits reveals that the deposits mainly contain partially melted submicron aerosols rich in K and S (see typical examples from spot 5-7 in Figure 14c) and spherical particles (normally 5-100 μm) rich in K, Si and Ca (see typical examples from spot 3 and 4 in Figure 14c).

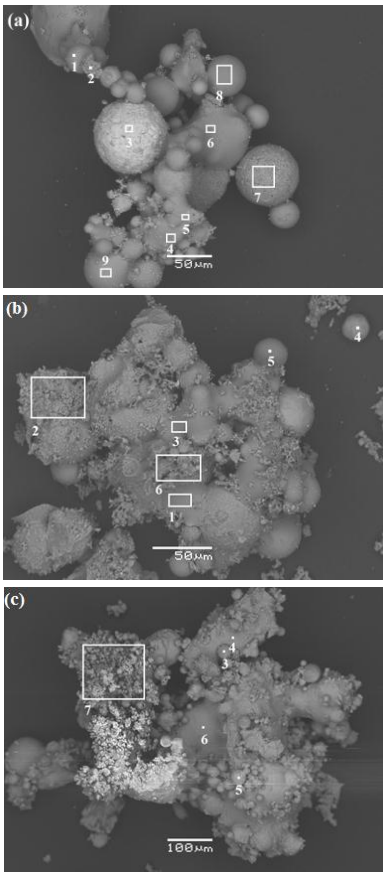

Figure 14: Typical SEM-EDS results of the deposits collected from the test without coal fly ash addition at Location A: (a) outer layer windward deposits, (b) inner layer windward deposits, (c) leeward deposits.

For the deposits collected at Location B during pulverized wood combustion, it is revealed that the major inorganic elements in the windward deposits are Ca and K, supplemented by smaller amounts of Cl, Fe, S, Si and

Mg. Compared to the windward deposits collected at Location A, the windward deposits at Location B are characterized by a significantly larger K, S and Cl content, and a much smaller Si content. The majority of the K (~88%) in the windward deposits at Location B is water soluble. The molar ratio of the water soluble (K+Na)/(Cl+2S) is about 2.44, indicating that a large fraction (~60%) of the water soluble alkalis may be hydroxides or carbonates. The molar ratio of water soluble S/Cl is about 0.94, meaning that an almost equal amount of alkali sulfates and chlorides in the windward deposits. SEM-EDS analyses of the windward deposits find a large quantity of small particles rich in K, Ca, S and Cl, which mostly present as clusters (see typical examples in Figure 15a). The leeward deposits at Location B show similar compositions as that of the windward deposits. A large content of the water soluble K is also seen in the leeward deposits. The molar ratio of the water soluble (K+Na)/(Cl+2S) is 1.74, suggesting that a large fraction (~40%) of the water soluble alkalis is hydroxides or carbonates. The malor ratio of water soluble S/Cl is about 1.33, implying that the amount of alkali sulfates and chlorides is comparable in the leeward deposits. On the other hand, the leeward deposits also contain some spherical Si-Ca rich particles (see typical examples from spot 3 and sport 4 in Figure 15b), which are generally not observed in the windward deposits collected at Location B.

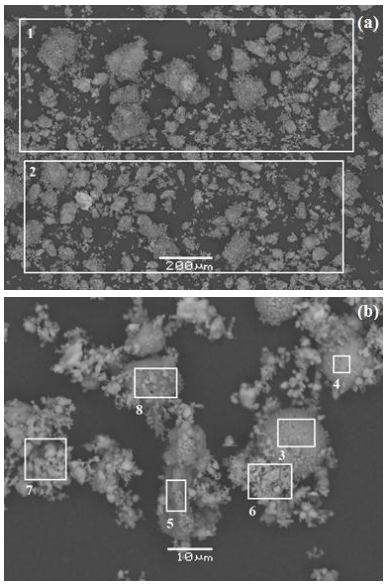

Figure 15: Typical SEM-EDS results of the deposits collected from the test without coal fly ash addition at Location B: (a) windward deposits, (b) leeward deposits.

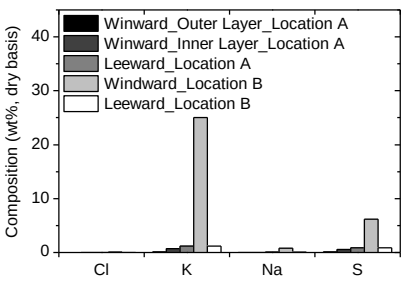

Figure 16: Water soluble compositions of the deposits collected during the tests with coal fly ash addition.

For the deposits collected during the tests with coal fly ash addition, only SEM-EDS analysis and water soluble composition analysis are performed. The results of the water soluble composition analysis are shown in Figure 16. It can be seen that the presence of water soluble elements is generally negligible for the deposits collected at Location A, except for the small amounts of water soluble K and S found in the inner layer of the windward deposits and in the leeward deposits. The results from SEM-EDS analysis indicate that the deposits at Location A are predominantly comprised of spherical ash particles with a large Si and Al content, which most likely originate from the added coal fly ash (see typical examples in Figure 17a). In the inner layer windward deposits and in the leeward deposits, a few partial-melted submicron particles with large K and S content are seen (see typical examples in Figure 17b), indicating the presence of a small amount of K_2SO_4.

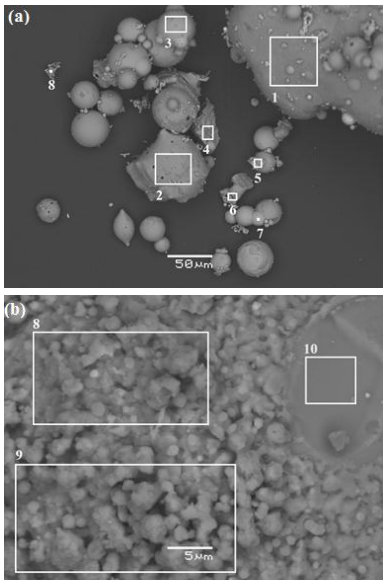

Figure 17: Typical SEM-EDS results of the deposits collected from the test with coal fly ash addition at Location A: (a) outer layer windward deposits, (b) leeward deposits.

The windward deposits collected at Location B exhibit a very large content of water soluble K and S (see Figure 16). The molar ratio of water soluble K/2S is about 1.7, suggesting the presence of both K_2SO_4 and KOH/K_2CO_3. SEM-EDS analysis confirms that the windward deposits at Location B primarily consist of agglomerated small particles with large K and S content (see typical examples from spot 4, 8 and 9 in Figure 18a), and a few small spherical ash particles (~2-3 μm) with large Si, Al and K content (see typical examples from spot 5-7 in Figure 18a). Compared to the windward deposits, the leeward deposits at Location B show significant lower content of water soluble K and S. This is supported by the SEM-EDS analysis, where the leeward deposits are found to be dominated by relatively large spherical particles rich in Si, Al and K (see typical examples in Figure 18b). These spherical particles usually have a size of ~2-20 μm and are probably originated from the added coal fly ash. Visual observation of the leeward deposits reveals that they are quite loose and can be removed very easily.

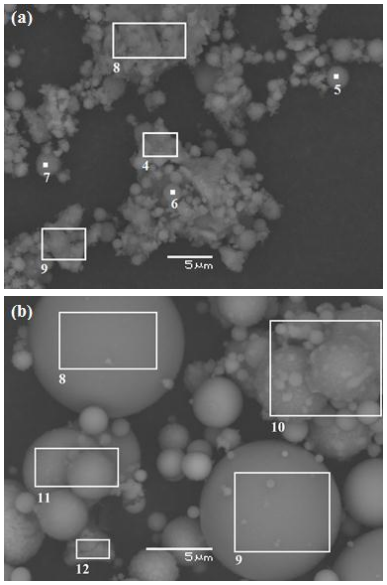

Figure 18: Typical SEM-EDS results of the deposits collected from the test with coal fly ash addition at Location B: (a) windward deposits, (b) leeward deposits.

3.7 Discussion of deposit formation mechanisms

During pulverized wood combustion, the primary ash deposition mechanism at Location A is the inertial impaction of the large (typically ~5-100 μm) Ca-Si-K rich spherical particles, which results in a large outer layer windward deposits that dominates the deposit mass. The K_2SO_4, KCl, and KOH/K_2CO_3 clusters found in the inner layer windward deposits or leeward deposits may be formed primarily through three mechanisms: (1) condensation of gaseous KCl and KOH; (2) reaction of the condensed KCl and KOH with SO_2 and/or CO_2 forming K_2SO_4 [21,22] and/or K_2CO_3 [6]; (3) thermophoresis of the KCl, KOH, K_2SO_4 and K_2CO_3 aerosols possibly generated by the large temperature gradient between the flue gas and the probe surface.

At Location B with low flue gas temperature, the windward deposits formed during pulverized wood combustion are probably deposited via condensation and/or thermophoresis of K_2SO_4, KCl, and KOH/K_2CO_3. Inertial impaction does not appear to be an important deposition mechanism, since large sperical particles rich in Si is generally not seen in the deposits. The leeward deposits at Location B have quite similar compositions as the windward deposits, excepting that some large Si-Ca rich particles are observed. This is most likely because when these particles hit the leedward side of the deposit probe, they are difficult to be removed through gravity shedding. A considerable amount of Cl is found in the deposits at Location B, most likely in the form of KCl, indicating that the degree of heterogeneous sulfation is not significant at Location B. This could be related to the relatively low flue gas temperature at this location, which may suppress the condensed sulfation reaction [21,22]. In addition, the SO_2 concentration may be very low at this location. According to thermodynamic calculations on woody fuels [23,24], SO_2 is found to be the only stable sulfur species at temperatures above 1200^{o}C. However, when the temperature is decreased from 1200^{o}C to 800^{o}C, the majority of the SO_2 would be converted to K_2SO_4. Such transformations may happen in the boiler, and result in a very low SO_2 concentration at Location B. This hypothesis is supported by the negligible SO_2 concentration measured downstream of Location B during the tests without coal ash addition (see Table III).

With the addition of a large amount of coal fly ash (~ 4 times of the mass of wood ash) to pulverized wood combustion, the KCl, K_2SO_4, and KOH in the flue gas are significantly reduced, as indicated by the obtained fly ash compositions (see Figure 4). Besides, the fly ash is dominated by the added coal fly ash. As a result, the deposits at Location A mainly comprise of Si-Al rich spherical particles that are deposited via inertial impaction. Compared to the test without coal fly ash addition, the amount of K_2SO_4 in the deposits is significantly decreased, although not completely removed. The presence of K_2SO_4 is probably because the added coal fly ash may not all the time fully remove the K_2SO_4, KCl and KOH in the flue gas. This is evident in full-scale aerosol measurements in the same boiler, where only in some tests a complete removal of KCl and K_2SO_4 was seen [10].

The deposits collected at Location B during coal ash addition are quite different from those obtained during pulverized wood combustion. Almost no Cl is found in the deposits collected during coal ash addition. This is partly linked to the reactions between the added coal fly ash and the KCl released from wood combustion, which can release the Cl as gaseous HCl. In addition, the SO_2 concentration in the flue gas is much higher during coal ash addition (see Table III). Therefore, even if small amount of KCl is deposited, they may be converted to K_2SO_4 through heterogeneous sulfation reactions, resulting in the K_2SO_4 clusters found in the deposits. A few K-Al-Si rich particles are found in the leedward deposits at Location B, which are generally quite loose deposits and can be removed easily.

4 CONCLUSION

Deposit formation during pulverized wood combustion was studied in a full-scale power plant by using an advanced probe system at two different boiler locations. At the location with high flue gas temperature (~1300^{o}C), the formation of deposits was characterized by a slow and continuous growth of deposits, followed by the shedding of a large layer of deposits that was most likely induced by the operation of soot-blowers in the boiler. The deposit formation appeared to be sensitive towards the wood properties, especially the content of Cl and S. The deposits formed contained primarily of Ca and Si rich spherical particles, and a considerable amount of K_2SO_4 was found at the inner layer windward deposits and the leeward deposits. At the location with low flue gas temperature (~800^{o}C), the deposit build up rate was relatively low and the amount of deposits on the probe became almost constant after a few hours. No major deposit shedding event was observed. The deposits at this location contained a relatively large amount of K_2SO_4, KCl and KOH/K_2CO_3.

The addition of a large amount of coal fly ash (~4 times of the mass of wood ash) greatly impacted the fly ash properties and its deposition behavior. The fly ash became dominated by spherical particles rich in Si and Al. The presence of KCl, K_2SO_4 and KOH in the flue gas was reduced significantly due to the reactions with the added coal fly ash. The deposit formation at the location with high flue gas temperature (~1300^{o}C) was characterized by a fast build-up of deposits, followed by

a frequent removal of a large layer of deposits. The formed deposits were dominated by the Si and Al rich particles originated from the coal fly ash. The presence of K_2SO_4 or other water soluble alkali species was generally negligible. At the location with low flue gas temperature (~800°C), the addition of coal fly ash did not change the ash deposition behavior significantly, but greatly affected the deposit properties. Almost no KCl appeared in the deposits, despite some K_2SO_4 and KOH/K_2CO_3 were still found.

The results from the present study imply that firing pulverized wood in a suspension-firing power plant may lead to corrosion problems in the boiler due to the presence of KCl in the flue gas that can generate deposits with relatively high Cl content. Firing pulverized wood with the addition of coal fly ash can effectively reduce or removal the KCl, and KOH/K_2CO_3 in the flue gas and in the deposits, thus reducing the corrosion risks. Although at high flue gas temperatures the ash deposition rate may be increased with coal fly ash addition, the deposit removal frequency is also increased and the deposit removal is often rather complete. Thus the addition of coal fly ash reduces ash deposition problems during pulverized wood combustion.

5 ACKNOWLEDGMENT

The work is part of the CHEC (Combustion and Harmful Emission Control) Research Centre. The financial support by DONG Energy Thermal Power A/S and The Danish Strategic Research Council (GREEN) is gratefully acknowledged.

6 REFERENCES

[1] The Danish Government. Our Future Energy. , 2011.
[2] van Lith SC, Alonso-Ramírez V, Jensen PA, Frandsen FJ, Glarborg P. Release to the gas phase of inorganic elements during wood combustion. Part 1: development and evaluation of quantification methods. Energy Fuels 2006;20:964-78.
[3] van Lith SC, Jensen PA, Frandsen FJ, Glarborg P. Release to the Gas Phase of Inorganic Elements during Wood Combustion. Part 2: Influence of Fuel Composition. Energy Fuels 2008;22:1598-609.
[4] Skrifvars BJ, Laurén T, Hupa M, Korbee R, Ljung P. Ash behaviour in a pulverized wood fired boiler-a case study. Fuel 2004;83:1371-9.
[5] Henderson P, Szakalos P, Pettersson R, Andersson C, Högberg J. Reducing superheater corrosion in wood-fired boilers. Materials and corrosion 2006;57:128-34.
[6] Blomberg T. Which are the right test conditions for the simulation of high temperature alkali corrosion in biomass combustion? Materials and Corrosion 2006;57:170-5.
[7] Zheng Y, Jensen AD, Johnsson JE. Deactivation of V2O5-WO3-TiO2 SCR catalyst at a biomass-fired combined heat and power plant. Appl Catal B-Environ 2005;60:253-64.
[8] Kling Å, Andersson C, Myringer Å, Eskilsson D, Järås SG. Alkali deactivation of high-dust SCR catalysts used for NOx reduction exposed to flue gas from 100MW-scale biofuel and peat fired boilers: Influence of flue gas composition. Applied Catalysis B: Environmental 2007;69:240-51.
[9] Wu H, Glarborg P, Frandsen FJ, Dam-Johansen K, Jensen PA. Dust-firing of straw and additives: ash chemistry and deposition behavior. Energy Fuels 2011;25:2862-73.
[10] Damoe AJ, Wu H, Frandsen FJ, Glarborg P, Sander B. Combustion aerosols from full-scale suspension-firing of wood pellets. Proceedings of the Impacts of Fuel Quality on Power Generation and the Environment, 2012, Puchberg, Austria.
[11] Sander B. Bioenergy for electricity and heat - experiences from biomass-fired CHP plants in Denmark. DONG Energy, 2007.
[12] Bashir MS, Jensen PA, Frandsen FJ, Wedel S, Dam-Johansen K, Wadenback J, Pedersen ST. Ash transformation and deposit build-up during biomass suspeinson and grate-firing: Full-scale experimental studies. Fuel Process Technol 2012;97:93-106.
[13] Bashir MS, Jensen PA, Frandsen FJ, Wedel S, Dam-Johansen K, Wadenback J, Pedersen ST. Suspension-firing of biomass. Part 1: Full-scale measurements of ash deposit build-up. Energy Fuels 2012;26:2317-30.
[14] Bashir MS, Jensen PA, Frandsen FJ, Wedel S, Dam-Johansen K, Wadenback J. Suspension-firing of biomass. Part 2: Boiler measurements of ash deposit shedding. Energy Fuels 2012;26:5241-55.
[15] International Flame Research Foundation. IFRF Suction Pyrometer, User Information Document.
[16] Zheng Y, Jensen PA, Jensen AD. A kinetic study of gaseous potassium capture by coal minerals in a high temperature fixed-bed reactor. Fuel 2008;87:3304-12.
[17] Wu H, Glarborg P, Frandsen FJ, Dam-Johansen K, Jensen PA, Sander B. Co-combustion of pulverized coal and solid recovered fuel in an entrained flow reactor – General combustion and ash behaviour. Fuel 2011;90:1980-91.
[18] Zheng Y, Jensen PA, Jensen AD, Sander B, Junker H. Ash transformation during co-firing coal and straw. Fuel 2007;86:1008-20.
[19] Robinson AL, Junker H, Baxter LL. Pilot-scale investigation of the influence of coal-biomass cofiring on ash deposition. Energy Fuels 2002;16:343-55.
[20] Hansen PFB, Andersen KH, Wieck-Hansen K, Overgaard P, Rasmussen I, Frandsen FJ, Hansen LA, Dam-Johansen K. Co-firing straw and coal in a 150-MWe utility boiler: in situ measurements. Fuel Process Technol 1998;54:207-25.
[21] Matsuda H, Ozawa S, Naruse K, Ito K, Kojima Y, Yanase T. Kinetics of HCl emission from inorganic chlorides in simulated municipal wastes incineration conditions. Chem Eng Sci 2005;60:545-52.
[22] Sengeløv LW, Hansen TB, Bartolomé C, Wu H, Pedersen KH, Frandsen FJ, Jensen AD, Glarborg P. Sulfation of Condensed Potassium Chloride by SO2. Energy Fuels 2013 (in press). doi:dx.doi.org/10.1021/ef400405z.
[23] van lith SC. Release of inorganic elements during wood-firing on a grate. PhD thesis, Department of Chemical Engineering, Technical University of Denmark, 2005.
[24] Sippula O, Lind T, Jokiniemi J. Effects of chlorine and sulphur on particle formation in wood combustion performed in a laboratory scale reactor. Fuel 2008;87:2425-36.